ELSEVIER

Bioelectrochemistry 57 (2002) 1–7

Bioelectrochemistry

www.elsevier.com/locate/bioelechem

Impedance analysis of ion transport through gramicidin channels in supported lipid bilayers

A.E. Vallejo [a], C.A. Gervasi [b,*]

[a] *Laboratorio de Ingeniería de Corrosión y Tecnología Electroquímica (LICTE), Facultad de Ingeniería, Universidad Nacional de La Plata, 1 y 47, 1900 La Plata, Argentina*

[b] *Instituto de Investigaciones Fisicoquímicas Teóricas y Aplicadas (INIFTA), Facultad de Ciencias Exactas, Universidad Nacional de La Plata, Sucursal 4, C.C. 16, 1900 La Plata, Argentina*

Received 10 April 2001; received in revised form 4 August 2001; accepted 26 September 2001

Abstract

Selectivity between monovalent cations and its sequence of conductivity in lipid bilayers doped with the antibiotic Gramicidin D (GD) were examined using EIS. Experiments were performed using lipid bilayers obtained from a lipid mixture of phosphatidylcholine and dimethyldioctadecylammonium chloride (DODAC). Lipid bilayers were supported on gold surfaces modified with a mercapto-carboxylic acid. The bilayers were formed by chemisorption of this last species to form the first monolayer on gold and subsequent fusion of unilamellar vesicles to form an external bilayer attached by electrostatic interactions. A mathematical expression for the impedance of the membrane processes was derived. Some predictions of the presented model were checked after fitting the experimental results in various electrolyte compositions. © 2002 Elsevier Science B.V. All rights reserved.

Keywords: EIS; Ion transport; Lipid bilayers; Gramicidin channels

1. Introduction

Artificial lipid bilayers have been employed extensively as model systems for studying biomembranes. The incorporation of reconstituted structures assembled from synthetic or natural molecules in lipid bilayers has enabled to explain important physiological processes such as transport, binding or charge transfer and have many potential applications. A diffused practical application is their use for biosensors with electrical detection, since they are able to interact specifically with certain species in solution.

Several systems emulating biological membranes, such as black lipid membranes [1] and membranes transferred via the Langmuir–Blodgett technique (Refs. [2,3] and references therein) or by fusion of vesicles [4,5] were analysed.

One of the most recent of these systems consists of planar supported membranes prepared by deposition of lipid monolayers onto a hydrophobic flat surface [6–8] or alternatively, by sequential transfer of a bilayer on a hydrophilic support by fusion of vesicles [9].

Several supports such as glassy-carbon, semiconductors [10] and salt bridges made of hydrogels in Teflon tubing, were considered. Alternatively, Tien et al. [11,12] demonstrated the spontaneous assembly of bilayer membranes on nascent metal surfaces, where an insulated metallic wire (e.g. a Teflon-coated Pt wire) is cut while immersed in a BLM-forming solution. Mercury was used to support gramicidin-modified phospholipid monolayers since the perfectly smooth and defect-free surface of the liquid electrode has some advantages over metal solid substrates [13].

Monolayers of alkanethiols on gold are most widely employed [14,15]. These monolayers allow deposition of a second monolayer [16,17] or bilayer on top of them, using several different preparation techniques [18]. Chemisorption of these compounds on clean gold generates monolayers, probably forming Au(I) thiolate(RS^-) species. This reaction may be considered as an oxidative addition of the S–H bond to the gold surface, followed by a reductive elimination of the hydrogen [7]:

$$R{-}S{-}H + Au_n^0 \rightarrow R{-}S^-Au^+ \cdot Au_n^0 + 1/2H_2.$$

A mercapto-carboxylic acid can be employed to obtain a negatively charged surface. When the carboxylic group is dissociated at the pH of the experiments, it supports a

* Corresponding author. Tel.: +54-221-425-7430; fax: +54-221-425-4642.

E-mail address: gervasi@inifta.unlp.edu.ar (C.A. Gervasi).

PII: S1567-5394(01)00127-X

negative charge. Subsequent addition and fusion of lipid vesicles generates electrostatic fixation of a bilayer.

In order to characterize ion transport across lipid membranes, de Levie et al. [19,20] developed a theoretical model for the transport impedance, although this model is restricted to the permeation of membrane-soluble ions across an ultrathin lipid bilayer separating two aqueous phases. However, in the literature, impedance results obtained with supported lipid bilayers containing pores or carriers that enable ion transport were analyzed either in terms of equivalent circuits [10] or in terms of adapted forms of the model of de Levie's [18,21]. At present, a theoretical impedance model for these specific cases is lacking.

One of the best characterized and most extensively studied pore-forming compound is gramicidin [22,23]. This linear pentadecapeptide consists of a helical dimer structure [24,25], which produces a continuous channel through a lipid bilayer. The resulting dimer has in its active form a length of 26 Å, sufficient to span a lipid bilayer. This peptide forms a pore of 4 Å in diameter allowing the passage of monovalent cations. Although the selectivity between these cations is not great, its sequence of conductivity was reported to be [26]: $H^+ > NH_4^+ > Cs^+ > Rb^+ > K^+ > Na^+ > Li^+$.

We report on experiments of fusion of vesicles into planar membranes on modified gold electrodes, thanks to electrostatic interaction between the charged surfaces of the substrate and the vesicles. This study was undertaken in order to show the applicability of impedance analysis to determine electric, chemical and physical parameters of these systems, which are of great importance in the biosensors field. The major goal of this work is the derivation of a theoretical impedance model dealing with ion transport through supported membranes containing the ion-channel-forming peptide Gramicidin D.

2. Materials and methods

2.1. Materials

Egg yolk phosphatidylcholine (eggPC), Thioglycollic acid (TGA) and Gramicidin D (GD) were obtained from Sigma. Dimethyldioctadecylammonium chloride (DODAC) was purchased from Fluka.

The Tris buffer, consisting of 10 mM Tris (tris-(hydroxymethyl)aminomethane) was adjusted to pH 7.4 by titration with HCl.

All aqueous solutions were prepared with Millipore water. All solutions were degassed before use.

2.2. Methods

2.2.1. Bilayer deposition by fusion of vesicles

Lipid vesicles were prepared by mechanical dispersion using a chloroform solution of a lipid mixture containing 80% and 20% w/w EggPC and positively charged DODAC, respectively. The solvent was removed by evaporation with nitrogen stream to avoid phospholipid oxidation. The dry film was shaken in a buffer solution (10 mM Tris, pH 7.4) with added GD to a final concentration of 0.001 M. The final concentration of the dispersion was 3%.

The self-assembled monolayer was formed by exposing the gold electrode to a 10-mM TGA solution for 10 min and next it was rinsed in the buffer solution to remove the unspecific adsorbed molecules. The carboxylic acid is dissociated at pH 7.4.

The negatively charged surface was immersed in the vesicle dispersion for 1 h and then it was dipped in the buffer solution to remove the remaining dispersion. For the experiments, the buffer solution was replaced by 0.1 M NaCl, LiCl, KCl and CsCl solutions in Tris 10 mM buffer pH 7.4.

2.2.2. EIS

The electrochemical cell in a three-electrode configuration contains a Ag/AgCl reference electrode, a large-area Pt counter electrode and the modified gold surface as the working electrode (0.28 cm^2 geometric area).

All measurements were carried out at the cell equilibrium voltage at 20 °C.

EIS data were measured with a Solartron SI 1254 device; a 10-mV amplitude sine-wave signal perturbation was applied in the 10 mHz–65 kHz frequency range. Data analysis was performed according to proper transfer function and identification procedures by using CNLS fit routines [27–29].

2.3. Theory

The mechanism under consideration involves aqueous diffusion that precedes two successive electrochemical steps leading to ion permeation through gramicidin-doped lipid bilayers.

Species M^+ arrives at the membrane/electrolyte interface by aqueous diffusion. After loosing its solvation shell, the cation adsorbs at a surface site corresponding to the mouth of an active G-channel and it incorporates into the channel at the interface. Since the incorporated ions are located at the membrane interface there is no physical distinction between adsorption onto the membrane and partitioning into it, and consequently no need to consider adsorption separately [20]. In the simplest case, the interfacial transfer kinetics are of first order.

For the permeation step we assume the validity of the single-barrier model, i.e. a simple activation energy barrier characterizes ionic transport inside the channels, and irreversible kinetics. It is also assumed that the applied voltage constitutes only a small perturbation of the barrier shape, so that the position of the potential-energy maximum along the reaction coordinate is not affected to any appreciable extent by the applied voltage.

The reaction mechanism can be formally written as:

$$M^+ \underset{k_{-1}}{\overset{k_1}{\rightleftarrows}} (M^+)^s \quad (1)$$

$$(M^+)^s \xrightarrow{k_2} (M^+)^e \quad (2)$$

where $(M^+)^s$ corresponds to the ion at the solution side of the membrane and $(M^+)^e$ to the ion at the electrode side of the membrane.

The potential (E) dependence of the rate constants can be expressed by an exponential law:

$$k_i = k_i^o \exp(b_i E) \quad (3)$$

$$k_{-i} = k_{-i}^o \exp(b_{-i} E) \quad (4)$$

where $b_i = -\alpha F/RT$ and $b_{-i} = (1-\alpha)F/RT$, k_i^o and k_{-i}^o are constants independent of E, α is the transfer coefficient and F the Faraday constant ($\approx 96\,500$ Cequiv^{-1}).

The maximum number of sites per unit surface which can be occupied by the species M^+ is characterized by the coefficient β and the fraction of sites actually occupied by θ ($0<\theta<1$). As a consequence the number of free electroactive sites is given by $\beta(1-\theta)$.

When the electrode potential is in the vicinity of the reversible potential of the considered reaction, the backward reaction of step (2) should a priori not be neglected. This in turn requires to consider a second fraction of sites θ occupied by the species $(M^+)^e$.

Mass and charge balances give:

$$\beta \frac{d\theta}{dt} = k_1(1-\theta)c - k_{-1}\theta - k_2\theta \equiv g(E,c,\theta) \quad (5)$$

$$I = FA[k_1(1-\theta)c - k_{-1}\theta + k_2\theta] \equiv I(E,c,\theta). \quad (6)$$

In order to calculate the reaction impedance, equations describing the rate of accumulation of incorporated ions $g(E,c,\theta)$ [Eq. (5)] and the current $I(E,c,\theta)$ [Eq. (6)] should be linearized, according to Taylor series expansion retaining only terms with first-order derivatives, giving:

$$\beta \frac{d\Delta\theta}{dt} = \left(\frac{\partial g}{\partial E}\right)\Delta E + \left(\frac{\partial g}{\partial \theta}\right)\Delta\theta + \left(\frac{\partial g}{\partial c}\right)\Delta c \quad (7)$$

$$\Delta I = \left(\frac{\partial I}{\partial E}\right)\Delta E + \left(\frac{\partial I}{\partial \theta}\right)\Delta\theta + \left(\frac{\partial I}{\partial c}\right)\Delta c. \quad (8)$$

Derivatives in Eqs. (7) and (8) correspond to stationary conditions and may be obtained from Eqs. (5) and (6).

When a small ac perturbation signal, $\Delta E = \tilde{E}\exp(j\omega t)$, is applied, the current and concentrations oscillate around steady-state values: $I = I^{dc} + \Delta I$, $c = c^{dc} + \Delta c$ and $\theta = \theta^{dc} + \Delta\theta$, where the superscript dc indicates a parameter that changes only slowly with time (i.e. either a steady-state term or one that does not change with the frequency of the perturbation ω), and the symbol Δ indicates a parameter oscillating periodically with time t. The resulting oscillations with time may be written as: $\Delta I = \tilde{I}\exp(j\omega t)$, $\Delta\theta = \tilde{\theta}\exp(j\omega t)$ and $\Delta c = \tilde{c}\exp(j\omega t)$.

Thus, Eqs. (7) and (8) can be rewritten as:

$$\beta j\omega \frac{\Delta\theta}{\Delta E} = \left(\frac{\partial g}{\partial E}\right) + \left(\frac{\partial g}{\partial \theta}\right)\frac{\Delta\theta}{\Delta E} + \left(\frac{\partial g}{\partial c}\right)\frac{\Delta c}{\Delta I}\left(-\frac{1}{Z}\right) \quad (9)$$

$$-\frac{1}{Z} = \frac{\Delta I}{\Delta E} = \left(\frac{\partial I}{\partial E}\right) + \left(\frac{\partial I}{\partial \theta}\right)\frac{\Delta\theta}{\Delta E} + \left(\frac{\partial I}{\partial c}\right)\frac{\Delta c}{\Delta I}\left(-\frac{1}{Z}\right) \quad (10)$$

where $Z = -\Delta E/\Delta I$ is the faradaic impedance (the negative sign arises from the assumed convention in which the cathodic current is positive).

Since species M^+ diffuses towards the surface, one has:

$$\frac{\Delta c}{\Delta I} = -\frac{N(\omega)}{FA} \quad (11)$$

where $N(\omega) = +\frac{1}{\sqrt{j\omega D}}$ for semi-infinite linear diffusion [30] and A represents the electrode area.

After eliminating $\Delta\theta$ from Eqs. (9) and (10) and considering Eq. (11), it results to:

$$Z = \frac{j\omega + \left(\frac{\partial I}{\partial c}\right)\frac{N}{FA}j\omega - \left[\left(\frac{\partial I}{\partial c}\right)\left(\frac{\partial g}{\partial \theta}\right) - \left(\frac{\partial I}{\partial \theta}\right)\left(\frac{\partial g}{\partial c}\right)\right]\frac{N}{FA}\frac{1}{\beta} - \left(\frac{\partial g}{\partial \theta}\right)\frac{1}{\beta}}{-\left(\frac{\partial I}{\partial E}\right)j\omega + \left[\frac{1}{\beta}\left(\frac{\partial I}{\partial E}\right)\left(\frac{\partial g}{\partial \theta}\right) - \frac{1}{\beta}\left(\frac{\partial I}{\partial \theta}\right)\left(\frac{\partial g}{\partial E}\right)\right]}. \quad (12)$$

After evaluating the derivatives in Eq. (12) from Eqs. (5) and (6) with $\alpha = 0.5$ and replacing θ by its steady state value, the final expression for the impedance can be obtained:

$$Z = \frac{j\omega + \frac{k_1 c + k_{-1} + k_2}{\beta} + \frac{k_1(k_{-1}+k_2)N}{k_1 c + k_{-1} + k_2}j\omega + \frac{2k_1k_2(k_{-1}+k_2)N}{\beta(k_1 c + k_{-1} + k_2)}}{\left[FA\frac{F}{RT}\frac{k_1 c(k_{-1}+k_2)}{k_1 c + k_{-1} + k_2}\right]j\omega + \frac{FA}{\beta}\frac{F}{RT}\frac{2k_1k_2c(k_{-1}+k_2)}{k_1 c + k_{-1} + k_2}}. \quad (13)$$

The approach presented is sufficient for analysing the electrochemical impedance, however, a simple check of some predictions of the proposed model can be made using a general equivalent circuit accounting for the expression of the global impedance. The procedure to obtain the equivalent circuit is based on a comparative analysis of the degree in ω of polynomial expressions for the numerator and denominator of the mathematical expression for Z given by Eq. (13) and that derived from the calculated impedance relative to the electrical circuit. According to the

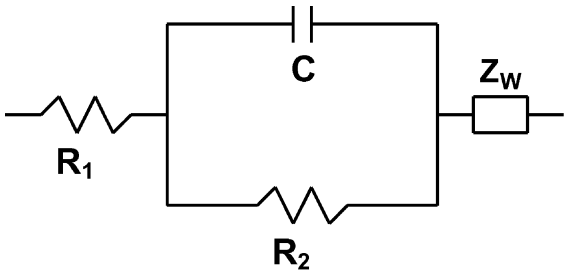

Fig. 1. Equivalent circuit accounting for the expression of the global impedance of the processes related to gramicidin-doped membranes.

equivalent circuit in Fig. 1, the electrochemical impedance is given by:

$$Z = \frac{j\omega + \dfrac{R_1 + R_2}{R_1 R_2 C} + \dfrac{Z_W}{R_1} j\omega + \dfrac{Z_W}{R_1 R_2 C}}{\dfrac{1}{R_1} j\omega + \dfrac{1}{R_1 R_2 C}} \tag{14}$$

where the element Z_W represents a Warburg impedance.

Comparison of terms of equal degree in ω in numerator and denominator of Eqs. (13) and (14) leads to the following relations between the electrical components R_1, R_2, C and Z_W and the kinetic parameters:

$$R_1 = \frac{k_1 c + k_{-1} + k_2}{FA\dfrac{F}{RT} k_1 c (k_{-1} + k_2)} \tag{15}$$

$$Z_W = \frac{1}{FA\dfrac{F}{RT}} \frac{1}{c} N \tag{16}$$

$$R_2 = \frac{R_1}{2}\left(\frac{k_1 c + k_{-1} + k_2}{k_2}\right) \tag{17}$$

$$C = \frac{\beta FA(F/RT) k_1 c (k_{-1} + k_2)}{(k_1 c + k_{-1} + k_2)^2}. \tag{18}$$

Finally, the impedance of the processes related to gramicidin-doped membranes consists of a parallel connection

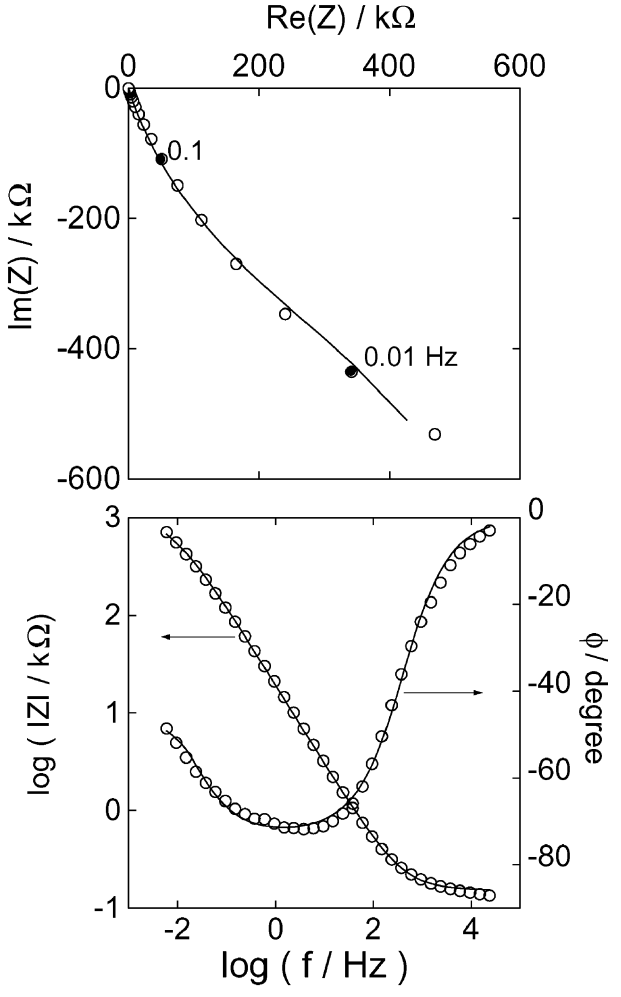

Fig. 2. Nyquist and Bode plots for a phospholipid-bilayer without added gramicidin in 0.1 M NaCl. Experimental data (○) and simulated curves (—) according to a transfer function determined by a constant phase angle (CPE) in parallel connection with a resistance.

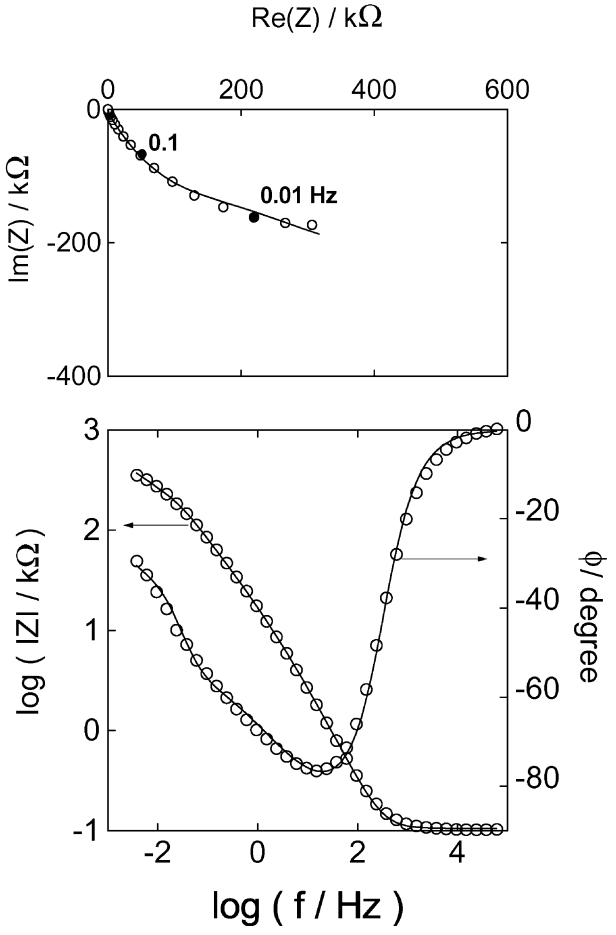

Fig. 3. Nyquist and Bode plots for a phospholipid-bilayer with added gramicidin in 0.1 M CsCl. Experimental data (○) and simulated curves (—) according to Eq. (14).

of the membrane capacitance C_m and the faradaic impedance Z.

3. Results and discussion

Fig. 2 shows impedance spectra of 0.1 M NaCl in Tris 10 mM buffer pH 7.4 at phospholipid-bilayer coated electrodes in the absence of gramicidin. It can be observed that $Z(\omega)$ becomes ohmic for $\omega \rightarrow 0$. This has been interpreted in the literature as due to the presence of defects in the bilayer [6]. These defects are most likely originated by the surface roughness of the gold substrate. This means that one has to introduce an additional resistance R_{defect} in parallel with the system's impedance to account for the small ohmic dc-currents associated to flawed areas at the coating. Experimental results in Fig. 2, after correction for the electrolyte resistance, were fitted to a constant phase element (CPE) in parallel connection with a resistance. Although the resulting theoretical response (continuous lines in Fig. 2) cannot describe the experimentally observed deflection of $\varphi(\omega)$ at $f \approx 1$ Hz, as reported for a comparable system [6], the fit was simply aimed at obtaining a rough estimation of $R_{defect} = 1.4 \times 10^6\ \Omega$ to be used as initial value in subsequent fits with doped lipid bilayers.

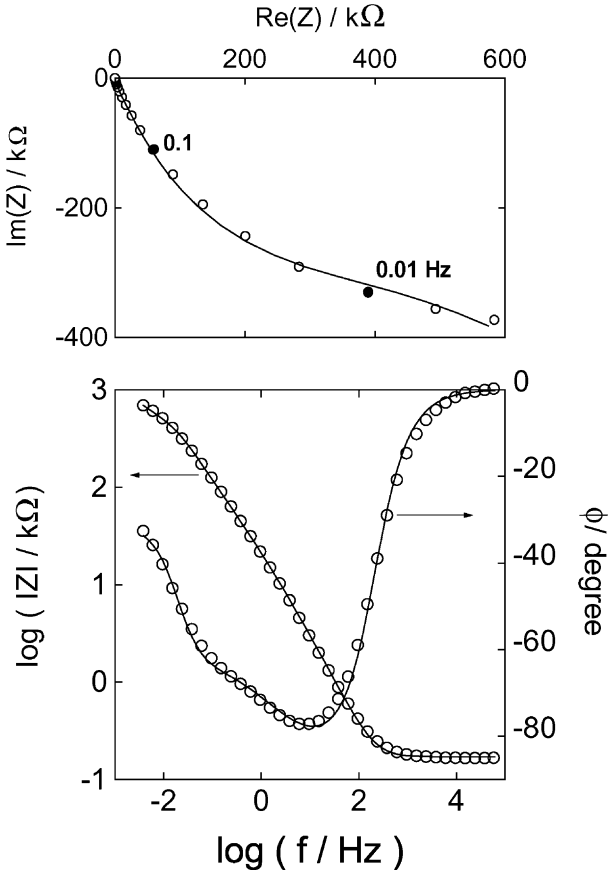

Fig. 4. Nyquist and Bode plots for a phospholipid-bilayer with added gramicidin in 0.1 M KCl. Experimental data (○) and simulated curves (—) according to Eq. (14).

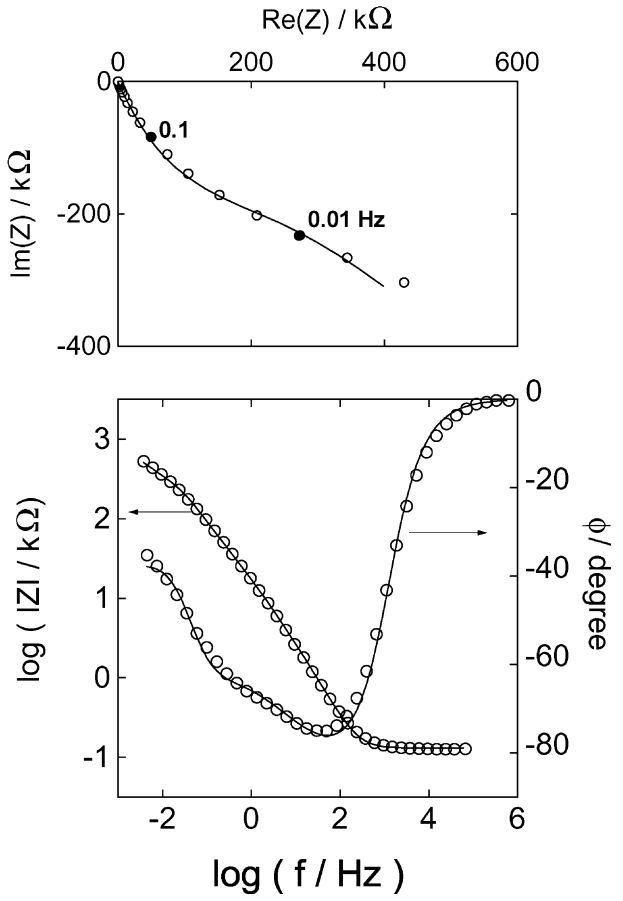

Fig. 5. Nyquist and Bode plots for a phospholipid-bilayer with added gramicidin in 0.1 M NaCl. Experimental data (○) and simulated curves (—) according to Eq. (14).

Figs. 3–6 display experimental and fitted impedance results for GD-doped bilayers in solutions containing Cs^+, K^+, Na^+ and Li^+, respectively.

Nyquist diagrams are characterized by a capacitive response with very little structure, containing at least two overlapped time constants. Accordingly, two overlapped phase maxima are present in the Bode plots. Aside from the differences in Z values, the spectra for the different solutions exhibit similar dynamic behaviour.

The continuous lines in Figs. 3–6 represent CNLS fits using the proposed model. A good agreement between experiment and theory can be observed in the whole frequency range. In the literature for similar systems fit predictions according to different models are ordinarily presented as log $|Z|$ vs. log ω, while the more sensitive variation of the phase angle φ with angular frequency ω is usually not included. Accordingly, it is not possible to compare the capability of our model to better describe the experiments with that of others.

It has been suggested that in order to account for the presence of a supporting monolayer a capacitance in series

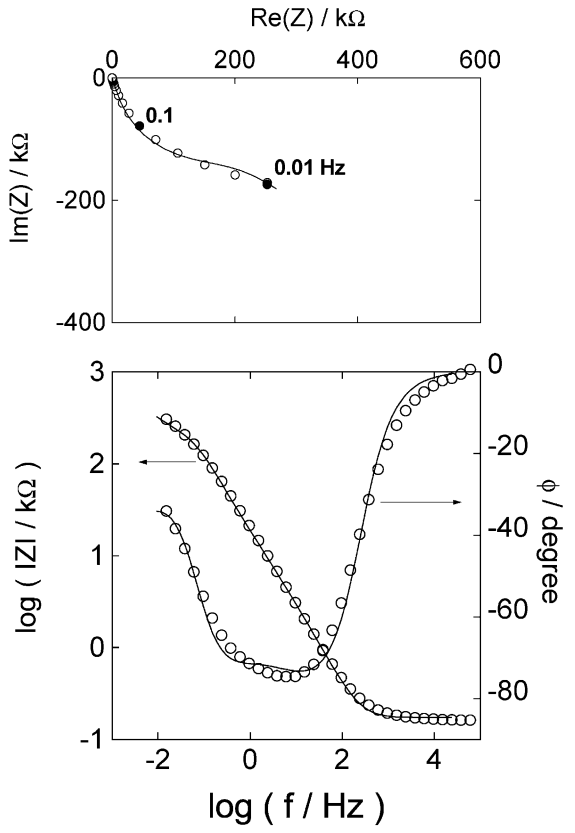

Fig. 6. Nyquist and Bode plots for a phospholipid-bilayer with added gramicidin in 0.1 M LiCl. Experimental data (○) and simulated curves (—) according to Eq. (14).

with the membrane impedance has to be added. To check this possibility we also fitted the results shown in Figs. 3–6, in that way, estimating a mean capacitance value $C_{TGA} = (8.4 \pm 0.9) \times 10^{-5}$ F cm^{-2}. As expected, this value is larger than that measured for thicker 3-mercaptopropionic acid monolayers [31]. However, considering C_{TGA} in the theoretical equations neither improves the quality of the fits nor influences appreciably the final values of the rest of the fitting parameters. Thus, to keep the analysis simple, we neglected C_{TGA}. Parameter estimates are assembled in Table 1.

Remarkably, the values derived for the ion transport resistance, which involves both transport across the interface and across the membrane $R_1 = R_{it} = -(\partial I/\partial E)^{-1}_{\theta,c}$, for the different cations in solution agree with the sequence of conductivity reported in the literature. On the other hand, R_1 is the only parameter that presents a marked dependence on the type of ion in solution.

Values of C due to adsorption processes were estimated to be, as expected, at least one order of magnitude larger than those of C_m.

The results shown indicate that the simplifying assumptions made in the theoretical derivation of the electrode impedance do not impose severe limitations for the successfull application of the model. However, two aspects deserve further discussion. First-order kinetics were assumed for the interfacial reactions. Recently, current–voltage characteristics for the ion transport through lipid bilayers containing short-lived water channels induced by thermal fluctuations were modelled considering the ion-pore coupling step as a second-order kinetic process that depends on both the ion concentration and the pore concentration [32]. This approach, which leads to an improved description of the experimentally observed deviation from an ohmic behaviour in the polarization curves at high potential values, could in principle be incorporated in our model. The second aspect is related to the assumed value of α. As usual, in the literature, a value $\alpha = 0.5$ was taken, although independent determination of its exact value from dc data is desirable to improve the agreement between theory and experiment.

At present, we are simulating the experimental data according to Eq. (13) in order to derive values for the kinetic constants and also to check the dependence of Z on temperature and cation concentration as predicted by the model. In principle, it may be possible to roughly estimate the density of conducting gramicidin dimers from the steady state values of θ at each applied dc-potential.

4. Conclusions

To avoid the weaknesses of analysing impedance data exclusively in terms of electrical analogs, we derived the mathematical expression of the transport impedance resulting from ion permeation in supported membranes containing ion-channel-forming peptides. CNLS fit of experimental data to the model allows to check the accepted sequence of conductivity. Further work based on the proposed theoretical model is expected to allow important predictions to be made as outlined above. We believe that this approach may be useful to characterize reconstituted

Table 1
Parameters obtained by CNLS fit routine of impedance data in Figs. 3–6 in terms of the transfer function Eq. (14)

	R_1/Ω	C_m/F	R_2/Ω	C/F	Y_0/Ω^{-1} s$^{-1/2}$	R_{defect}/Ω
Li^+	69	3.72×10^{-6}	1.46×10^5	1.47×10^{-5}	1.56×10^{-5}	4.94×10^6
Na^+	20	4.60×10^{-6}	1.19×10^5	4.23×10^{-5}	1.44×10^{-5}	8.72×10^6
K^+	8.8	4.40×10^{-6}	2.30×10^5	3.28×10^{-5}	0.99×10^{-5}	3.93×10^6
Cs^+	0.2	4.68×10^{-6}	0.70×10^5	7.70×10^{-5}	1.44×10^{-5}	1.19×10^6

The electrolyte resistance was $R_e = 150\ \Omega$. Parameter Y_0 is related to the Warburg coefficient through $Z_W = 1/Y_0(j\omega)^{1/2}$.

protein/lipid systems, in studies of membrane interfacial phenomena and in sensor applications.

References

[1] S. Alonso-Romanowski, L.M. Gassa, J.R. Vilche, An investigation by EIS of gramicidin channels in bilayers lipid membranes, Electrochim. Acta 40 (1995) 1561–1567.

[2] K.B. Blodgett, I. Langmuir, Built-up films of barium stearate and their optical properties, Phys. Rev. 51 (1937) 964–971.

[3] J.A. Zasadzinski, R. Viswanathan, L. Madsen, J. Garnaes, D.K. Schwartz, Langmuir–Blodgett films, Science 263 (1994) 1726–1733.

[4] S. Alonso-Romanowski, A.E. Vallejo, L.M. Gassa, J.R. Vilche, Identification of channel membrane processes in bilayer lipid membranes by electrochemical techniques, Bioelectrochem. Bioenerg. 42 (1997) 187-192.

[5] A.E. Vallejo, C.A. Gervasi, L.M. Gassa, Temperature dependence of ionic transport through gramicidin A channels in liposomes: an EIS study, Bioelectrochem. Bioenerg. 47 (1998) 343–348.

[6] M. Stelzle, G. Weissmüller, E. Sackmann, On the application of supported bilayers for biosensors with electrical detection, J. Phys. Chem. 97 (1993) 2974–2981.

[7] A. Ulman, Formation and structure of self-assembled monolayers, Chem. Rev. 96 (1996) 1533–1554.

[8] H. Lang, C. Duschl, M. Grätzel, H. Vogel, Self-assembly of thiolipid molecular layers on gold surfaces: optical and electrochemical characterization, Thin Solid Films 210/211 (1992) 818–821.

[9] E. Kalb, S. Frey, L.K. Tamm, Formation of supported planar bilayers by fusion of vesicles to supported phospholipid monolayer, Biochim. Biophys. Acta 1103 (1992) 307–316.

[10] S. Gritsch, P. Nollert, F. Jähnig, E. Sackmann, Impedance spectroscopy of porin and gramicidin pores reconstituted into supported lipid bilayers on indium–tin oxide electrodes, Langmuir 14 (1998) 3118–3125.

[11] H.T. Tien, Z. Salamon, Formation of self-assembled lipid bilayers on solid substrates, Bioelectrochem. Bioenerg. 22 (1989) 211–217.

[12] T. Martynski, H.T. Tien, Spontaneous assembly of bilayer membranes on a solid surface, Bioelectrochem. Bioenerg. 25 (1991) 317–324.

[13] M. Rueda, I. Navarro, G. Ramirez, F. Prieto, C. Prado, A. Nelson, Electrochemical impedance study of Tl^+ reduction through gramicidin channels in self-assembled gramicidin-modified dioleoylphosphatidylcholine monolayers on mercury electrodes, Langmuir 15 (1999) 3672–3678.

[14] A. Plant, Self-assembled phospholipid/alkanethiol biomimetic bilayers on gold, Langmuir 9 (1993) 2764–2767.

[15] P. Krysinski, M. Brzostowska-Smolska, Capacitance characteristics of self-assembled monolayers on gold electrode, Bioelectrochem. Bioenerg. 44 (1998) 163–168.

[16] J. Ha, Ch. Henry, I. Fritsh, Formation and characterization of supported hexadecanethiol/dimyristoyl phosphatidylcholine hybrid bilayers containing gramicidin D, Langmuir 14 (1998) 5850–5857.

[17] L. Ding, J. Li, S. Dong, E. Wang, Supported phospholipid membranes: comparison among different deposition methods for a phospholipid monolayer, J. Electroanal. Chem. 416 (1996) 105–112.

[18] C. Steinem, A. Janshoff, W.P. Ulrich, M. Sieber, H.-J. Galla, Impedance analysis of supported lipid bilayer membranes: a scrutiny of different preparation techniques, Biochim. Biophys. Acta 1279 (1996) 169–180.

[19] S.K. Rangarajan, P.F. Seelig, R. de Levie, On the admittance of lipid bilayer membranes, J. Electroanal. Chem. 100 (1979) 33–62.

[20] R. de Levie, Mathematical modeling of transport of lipid-soluble ions and ion-carrier complexes through lipid bilayer membranes, Adv. Chem. Phys. 37 (1978) 99–137.

[21] C. Steinem, A. Janshoff, K. von dem Bruch, K. Reihs, J. Goossens, H.-J. Galla, Valinomycin-mediated transport of alkali cations through solid supported membranes, Bioelectrochem. Bioenerg. 45 (1998) 17–26.

[22] S.B. Hladky, D.A. Haydon, Ion transfer across lipid membranes in the presence of gramicidin A, Biochim. Biophys. Acta 274 (1972) 294–312.

[23] W. Veatch, L. Stryer, The dimeric nature of the gramicidin A transmembrane channel: conductance and fluorescence energy transfer studies of hybrid channel, J. Mol. Biol. 113 (1977) 89–102.

[24] D.W. Urry, M.C. Woodall, J.D. Glickson, D.F. Mayers, Proc. Natl. Acad. Sci. U. S. A. 68 (1997) 1907.

[25] D.W. Urry, Proc. Natl. Acad. Sci. U. S. A. 68 (1971) 672.

[26] V.B. Myers, D.A. Haydon, Ion transfer across lipid membranes in the presence of gramicidin A, Biochim. Biophys. Acta 274 (1972) 313–322.

[27] R.H. Milocco, E.B. Castro, S.G. Real, J.R. Vilche, in: W.H. Smyrl, D.D. Macdonald, W.J. Lorenz (Eds.), Corrosion Science and Engineering, The Electrochemical Society, Pennington, NY, 1989, pp. 88–101.

[28] E.B. Castro, S.G. Real, R.H. Milocco, J.R. Vilche, The application of electrochemical impedance spectroscopy and identification procedures to the investigation of the dissolution and passivation of iron in carbonate–bicarbonate buffers at 25 °C, Electrochim. Acta 36 (1991) 117–126.

[29] C.A. Gervasi, J.R. Vilche, An impedance spectroscopy study of the anodically formed barrier layer on Al substrates, Electrochim. Acta 37 (1992) 1389–1394.

[30] C. Gabrielli, Identification of Electrochemical Processes by Frequency Response Analysis, Technical Report No. 004, Solartron, Hampshire, UK, 1984.

[31] C. Steinem, A. Janshoff, H.-J. Galla, M. Sieber, Impedance analysis of ion transport through gramicidin channels incorporated in solid supported lipid bilayers, Biolectrochem. Bioenerg. 42 (1997) 213–220.

[32] F. Bordi, C. Cametti, A. Naglieri, Ionic transport in lipid bilayer membranes, Biophys. J. 74 (1998) 1350–1370.